

Estimation and Analysis of Thermal Response of Human Tissue during EM Exposure

M. Prishvin¹, L. Bibilashvili¹, R. Zaridze¹, A. Mohammad², and R. Islam²

¹ Laboratory of Applied Electrodynamics, Tbilisi State University, Tbilisi, 0128, Georgia

² University of South Carolina, USA
prishvin@gmail.com

Abstract. During last decades, the environment has undergone serious changes from EM point of view. An objective of this paper is to analyze realistic exposure scenarios by means of numerical computations. Our aim is to determine peak values of SAR and temperature rise in various scenarios. This paper contains results of computer simulations performed on a human model [1] with and without consideration of detailed blood perfusion in the model [2].

1 Introduction

The recent results of the study on numerical simulations of electromagnetic (EM) exposure of human body by wireless transmitters are discussed in this paper. To date, a large number of dipole, monopole, and PIFA antennas were studied at different frequencies and distances to quantify the SAR level produced in the human body. The present study expands this work by simulating the temperature rise in human body related to those exposure conditions. The thermal simulations were conducted using the proprietary program package, which was developed in our Laboratory – FDTDLab [3-5] in cooperation with Motorola Inc (2002-2008). Validation of FDTDLab was proved for EM and thermal solutions part using different ways [4, 5]. The software package was enhanced with several new features including the calculation of peak values in selected tissue regions and/or tissue, and most importantly the consideration of directional blood flow in the tissue capillary and its effect on the special distribution of the temperature and temperature rise in the Human model [1].

Part of this work was conducted within MMF Phase II project. Our aim was to investigate EM exposure and determine peak SAR and temperature rise values in various scenarios without consideration of directional blood flow. Modified bio-heat equation and vascular structure generation algorithm is introduced for more advanced simulation method currently under development [2]. The task included: use of the Finite Difference Time Domain (FDTD) method and anatomically based human head models; computation the peak 1-g and 10-g averaged SAR [6-9] and the temperature rise in the tissue for canonical dipole antennas of various length ($\lambda/2$, $\lambda/4$, $\lambda/8$ and at 300, 450, 900, 1450, 1900, 2450, 3700 and 6000 MHz and at distances of 5, 10 and 20 mm from the head model. The 1-g and 10-g averaged-SAR distributions were subsequently computed on the basis of the algorithm specified in IEEE C95.3-2002 standard (IEEE, 2002) (2002) [7-9].

2 Materials and Methods

The simulations were conducted using the FDTD method. Temperature increase in tissue was simulated due to RF exposure from antennas placed at different distances from the head models. The EM and thermal coupled solver FDTDLab, developed at TSU [4, 5], was used. As it is shown in [5] the thermal solver is tested against an analytical solution for a simplified case. At the initial phase of the project various standard antenna and phantom orientations were simulated. Along with the SAR the conventional bio-heat model was used to compute temperature rise and then more advance thermal model that includes the directional blood flow information and then newly developed method that generates vascular structure geometry and blood flow velocity field was also used for heat exchange simulations in those conditions. The difference between the conventional and advance model has been observed and analyzed.

A new algorithm for construction of realistic vessel networks, blood flow velocity vectors and a new approach to simulate heat exchange in tissue during EM exposure considering heat convection by blood was implemented in FDTDLab software. Heat exchange in tissue is calculated according to the modified Pennes equation [2]. The distinctive feature of the new approach is that the blood perfusion and temperature is not constant through the model. Blood flow velocity vector field is defined together with the geometry and remains unchanged during simulations while blood temperature is calculated at every point in the model based on approximated heat exchange mechanism with tissue. As a result a non-constant blood temperature is obtained during simulations and new tissue temperature and temperature rise has been produced which appear to be slightly lower than the tissue temperature computed using conventional Pennes bio-heat model. The new blood flow model also produces different temperature rise distribution with the hot spots at slightly different locations compared to the conventional model.

3 Dipole Antennas

On Fig. 1 dependencies of peak 10g SAR and temperature rise on frequency are shown. As it can be seen from Fig. 1a and Fig. 1b minimal SAR and temperature rise for dipole antennas are observed around 900MHz. Due to complexity of the model and frequency dependent material properties, points of maximal SAR and temperature rise are located in different parts of the head and may not correspond to each other (Fig. 2). As a result graphs are not smooth and it is harder to make conclusions based on them. Since at lower frequencies field penetration depth is significantly deeper, peak values of SAR and temperature rise for inner parts of the model (e.g. brain, eye, etc.) are much higher for lower frequencies.

Starting from 1450 MHz the penetration depth of EM field is small and biggest part of radiated energy is absorbed at the surface, which in the studied model in most cases is the ear.

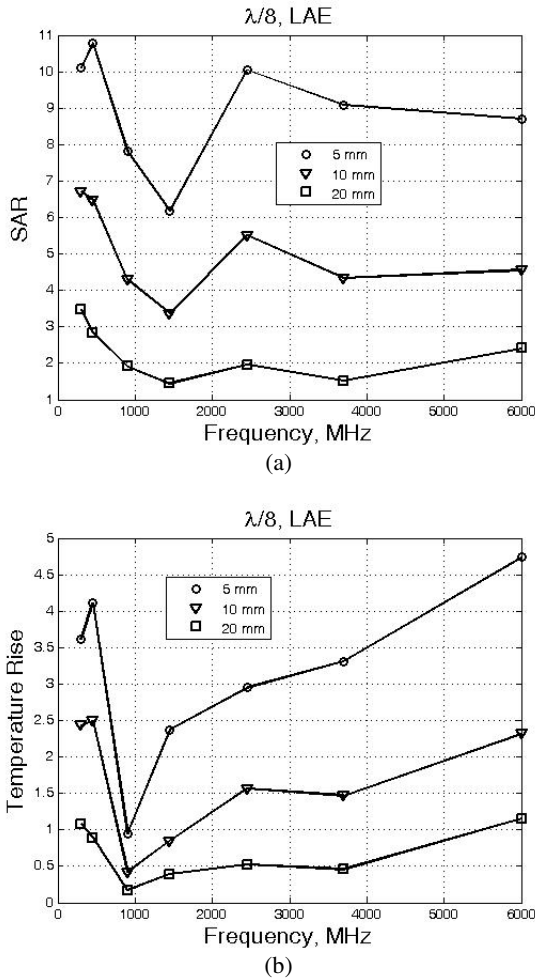


Fig. 1. (a) SAR on frequency. All data normalized to input power, (b) Temperature rise on frequency. All data normalized to input power.

As it can be seen from Fig. 2 location of peak temperature rise and SAR depend on particular case and may not correspond to each other. In this case match only locations of peak 1g SAR and temperature rise while the location of peak 10g SAR is in another part of the model. The geometry of the antenna and its placement can drastically affect resultant distributions of SAR and temperature rise.

The complexity of the geometry makes hard to predict the location of peak values and compare their values. When the field penetration depth is comparable with the linear dimensions of the model, a focusing effect can be observed Fig. 3.

As a result in order to obtain correct results the location of the dipole should be chosen in order to avoid focusing effects. But, if the position of device is changed during the communication process, the peak values are washed out and the impact could be smaller.

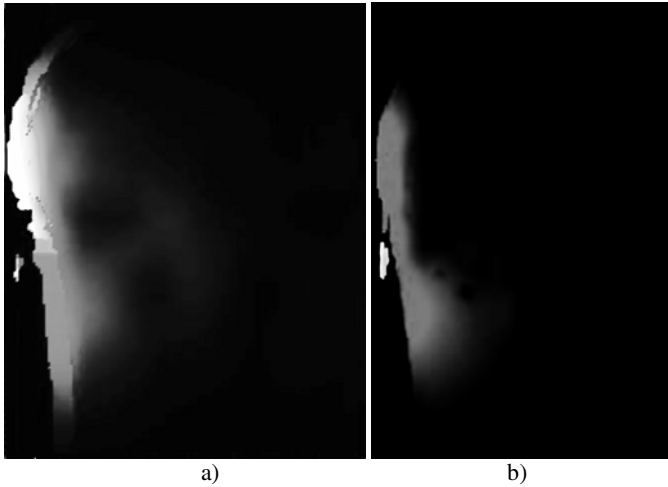


Fig. 2. Locations of peak a) $10\text{g SAR} = 6.7\text{w/kg}$ b) temperature rise $\Delta T = 0.36^\circ\text{C}$ of $\lambda/8$ -th Dipole Antenna for frequency 300 MHz, at 10 mm distance

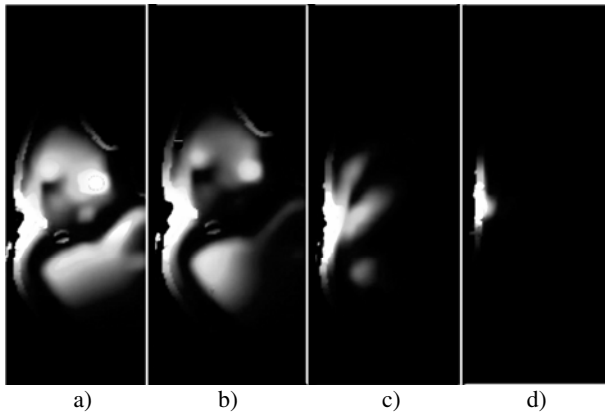


Fig. 3. Field penetration depth for $\lambda/2$ -th dipole antennas. 1g SAR with frequencies: a) 300 MHz b) 450 MHz c) 1450 MHz and d) 3700 MHz.

4 Monopole Antennas

Resonant monopole antennas operating at (300, 900, 1450, and 1900) MHz were investigated in terms of this project. Temperature rise and SAR was the subject of study in all calculations. Antennas were placed at distances of 10 and 20 mm from the Duke Head model [1]. Three types of monopoles namely; the straight, the helical and the meander were mounted on top of a metal box. Simulations at 900 and 1900 MHz were done using XFDTD (at USC) while those at 300 and 1450 MHz were done using FDTDLab (at TSU).

A 1 mm uniform discretization was used. Each monopole was excited using a 1 mm gap excitation with a continuous wave sinusoidal source at corresponding frequency. All SAR and temperature rise data were normalized to 1W of power. The SAR and temperature rise data reflect the maximum absorption of power by the specific antenna under consideration. In XFDTD eight layers of PML were employed as absorbing boundaries in FDTDLab seven layers were used.

As it was expected, both SAR and temperature values decrease with the increase of distance. Since tissue thermal parameters like specific heat, heat conductivity, blood perfusion etc. are independent of frequency the temperature rise depends only on SAR. At fixed frequency SAR and temperature rise are in good correlation. Peak temperature rise values induce by different antennas may appear in different parts of the model (e.g. some are located in the earlobe while other may appear above the ear or in its middle). The maximal temperature rise $\Delta T=0.99^{\circ}\text{C}$ and maximal 10g SAR=10.5 W/kg were observed at 1900 MHz for 10mm helical monopole. The minimal temperature rise $\Delta T=0.21^{\circ}\text{C}$ was observed at several frequencies. Minimal peak 10g SAR was observed at 300MHz for straight monopole located at 20mm distance from the model.

It was noted the due to the complexity of the geometry and a asymmetrical radiation pattern of the antennas location of peak temperature rise and peak 10g SAR may not match. This fact makes analysis of SAR and T-rise correlation harder (Fig.2).

It was observed that in some 20mm the points of maximal temperature rise and 10g SAR match while at 10mm they do not. In such cases it is hard to expect good correlation between temperature rise and SAR.

5 PIFA Antennas

The second task consisted in examination of planar inverted-F antennas (PIFA) operating at, 1900 , 3700, and 6000 MHz. Antennas were placed at distances of 10 and 20 mm from the Duke head model. Two different orientations of the PIFA namely the conventional and the flipped were used. Simulations at 1900, 3700 and 6000 MHz were conducted using FDTDLab (at TSU). The distance „d” is calculated as the separation between the outer edge of the compressed ear and the surface of the metal box facing the metal strip of the PIFA. The time step for thermal calculations was 0.5 second for all antennas. The basal body temperature was considered as 37°C . Air at 23°C with a thermal conductivity of $0.026 \text{ Watt/meter}/^{\circ}\text{C}$ was used as the immersive medium.

The maximal temperature rise $\Delta T=4.68^{\circ}\text{C}$ and maximal 10g SAR = 8.41 W/kg were observed at 6000 MHz 10mm PIFA antenna with flipped orientation. The minimal temperature rise $\Delta T=0.21^{\circ}\text{C}$ was observed at 1900MHz for PIFA antenna with conventional orientation located at 20mm distance from the model.

Good correlation between SAR and temperature rise was observed at all frequencies. Although the temperature rise of 4.68°C is high enough the resultant maximal temperature does not exceed 37°C . While conducting the calculations it was noted that antenna position may drastically affect resultant peak values of SAR and temperature rise and corresponding distributions.

The maximum ΔT exhibits a strong correlation with both peak 1-g avg. SAR and peak 10-g avg. SAR. Fig. 4 shows the peak ΔT values for the 1900, 3700 and 6000 MHz PIFAs plotted against the 10-g avg. SAR. Similar dependency is observed for 1g SAR. [10-12].

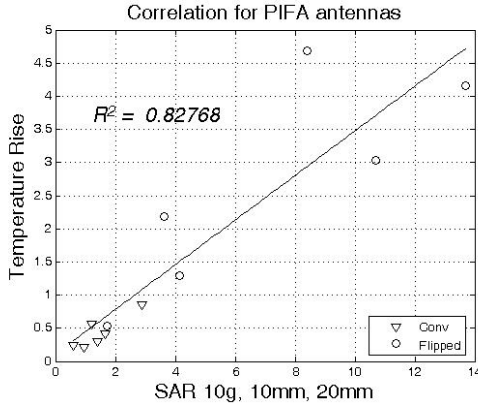


Fig. 4. Correlation between 10g SAR and temperature rise at 1900, 3700, 6000 frequencies

6 Additional Notes

The software package FDTDLab was enhanced with several new features. A new model of blood perfusion with directional capillary blood flow [2] taken into account was added to it along with such features like analyzing peak values for temperature rise and SAR for selected tissues and regions.

While the difference produced by two models was noticed, the thorough analysis is needed to quantify it. As an example the Fig. 5 shows the difference in temperature rise distribution computed for the same exposure condition using the conventional and new heat-exchange model.

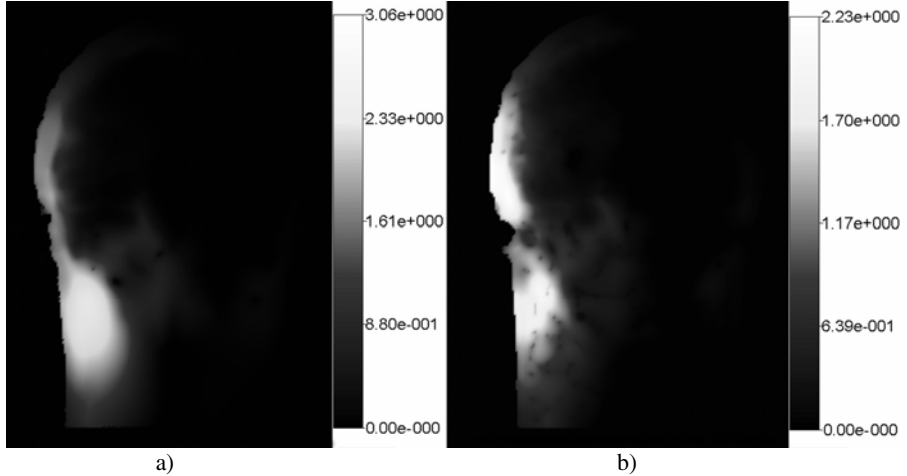


Fig. 5. Temperature rise for: a) Pennes model and b) modified model with new vascular structure model. SAR normalized to 1W input power.

Both models considered in this study are restricted to low power exposure conditions but may be extended to higher power levels by introducing reported in literature approximations of the basic thermal regulation mechanisms.

The modified model [2] is linear, and there is good correlation between peak 10g SAR values peak temperature rise values calculated according to it. At Fig. 5 calculations according to the modified model are presented. Fig. 5a shows temperature distribution according to conventional bio-heat equation, Fig. 5b distribution obtained according to the modified equation [2]. The darker parts correspond to venous endings while the lighter areas to arterial endings where the blood penetrates into examined volume.

In addition to the described calculations using the Visible Human Model [1] a simplified model has been studied. [10],[11]. It appeared that presence of a hand affects the radiation pattern and the resultant SAR and temperature distributions.

7 Conclusions

Dipole, monopole, planar inverted-F antennas operating at 1900, 3700 and 6000 MHz were investigated. Peak values of specific absorption rate (SAR) and induced temperature rise in the Duke Head model were presented. Peak temperature rise ranged from 0.1°C to 4.7°C for all the antennas considered. Antennas in the flipped orientation in general induced much higher temperature rise than in the conventional. It was shown that geometry of the model and antenna radiation pattern drastically affects the resultant distributions of SAR and temperature rise [11]. In some cases peak values of SAR and/or temperature rise may change by 70% if antenna is shifted by 10mm in a plain parallel to the surface. This fact makes analysis much harder and in order to obtain valuable results each antenna at each distance should be studied separately.

References

1. Kuster, N.: IT'IS Foundation, <http://www.itis.ethz.ch/>
2. Prishvin, M., Manukyan, L., Zaridze, R.: Vascular Structure Model for Improved Numerical Simulation of Heat Transfer in Human Tissue. In: 20th International Zurich Symposium on Electromagnetic Compatibility, Zurich, Switzerland, January 12-16, pp. 261–264 (2009)
3. Bijamov, A., Razmadze, A., Shoshiashvili, L., Zaridze, R., Bit-Babik, G., Faraone, A.: Software for the electro-thermal simulation of the human exposed to the mobile antenna radiation. In: Proceedings of VIII-th International Seminar/Workshop on Direct and Inverse Problems of Electromagnetic and Acoustic Wave Theory (DIPED 2003), Lviv, Ukraine, September 23-25, pp. 173–176 (2003), <http://www.ewh.ieee.org/soc/cpmt/ukraine/>
4. Zaridze, R.S., Gritsenko, N., Kajaia, G., Nikolaeva, E., Razmadze, A., Shoshiashvili, L., Bijamov, A., Bit-Babik, G., Faraone, A.: Electro-Thermal Computational Suit for Investigation of RF Power Absorption and Associated Temperature Change in Human Body. In: 2005 IEEE AP-S International Symposium and USNC/URSI National Radio Science Meeting, Washington DC, USA, July 3-8, pp. 175–178 (2005)

5. Shoshiashvili, L., Razmadze, A., Jejelava, N., Zaridze, R., Bit-Babik, L.G., Faraone, A.: Validation of numerical bioheat FDTD model. In: Proceedings of XIth International Seminar/Workshop on Direct and Inverse Problems of Electromagnetic and Acoustic Wave Theory (DIPED 2006), Tbilisi, Georgia, October 11-13, pp. 201–204 (2006)
6. Islam, M.R., Razmadze, A., Zaridze, R., Bit-Babik, G., Ali, M.: Computed SAR and Temperature Rise in an Anatomical Head Model by Canonical Antennas. In: BEMS Annual Meeting, BEMS 2009 Congress Centre, Davos, Switzerland, June 14-19 (2009), <http://bioem2009.org/technical-program/>
7. Zaridze, R., Razmadze, A., Shoshiashvili, L., Kakulia, D., Bit-Babik, G., Faraone, A.: Influence of SAR Averaging Schemes on the Correlation with Temperature Rise in the 30-800 MHz Range. In: EUROEM 2008 European Electromagnetics, Swiss Federal Institute of Technology (EPFL), Lausanne, Switzerland, July 21-25, p. 120 (2008)
8. Bernardi, et al.: Specific Absorption Rate and Temperature Increases in the Head of a Cellular-Phone User. *IEEE Trans. Microwave Theory Tech.* 48(7), 1118–1126 (2000)
9. Razmadze, A., Shoshiashvili, L., Kakulia, D., Zaridze, R.: Influence on averaging masses on correlation between mass-averaged SAR and temperature rise. *Journal of Applied Electromagnetism* 10(2), 8–21 (2008), <http://jae.ece.ntua.gr/JAE> (December 2008/SAR and temperature rise Zaridze Paper 2.doc.pdf)
10. Mazmanov, D., Manukyan, L., Kakulia, D., Razmadze, A., Shoshiashvili, L., Zaridze, R.: MAS based software for the solving of diffraction and SAR problems on unbounded objects. In: Proceedings of XIth International Seminar/Workshop on Direct and Inverse Problems of Electromagnetic and Acoustic Wave Theory (DIPED 2006), Tbilisi, Georgia, October 11-13, pp. 11–16 (2006)
11. Zaridze, R., Prishvin, M., Tabatadze, V., Kakulia, D.: Hand Position Effect on SAR and Antenna Pattern in RF Exposure Study of a Human Head Model. In: BEMS 2009 Congress Centre, Davos, Technical Program, Switzerland, June 14-19 (2009), <http://bioem2009.org/technical-program>